

RESEARCH

Open Access

Modeling and simulation of an industrial secondary reformer reactor in the fertilizer plants

Ali Ashour AL-Dhfeery* and Ala'a Abdulrazaq Jassem

Abstract

In this paper, the industrial secondary reformer reactor has been modeled and simulated at steady-state operation conditions. It aims to modify a complete mathematical model of the secondary reformer design. The secondary reformer is a part of a subprocess in a higher scale unit of ammonia synthesis. It is located after the primary reformer in the ammonia plant where it is used in the synthesis of ammonia. The reactions in the secondary reformer reactor are assumed to be carried inside two reactors in series. The first reactor, upper section, is the combustion zone, while the second reactor, bottom section, is the catalyst zone with nickel catalyst based on the alumina. In order to create a reactor design model for the secondary reformer in the industrial ammonia plant, combustion and catalyst zones have been studied. The temperature and compositions of gas in the combustion zone are predicted using the atomic molar balance and adiabatic flame temperature model. In the catalyst zone, the temperature and composition profiles along the axial distance are predicted using a one-dimensional heterogeneous catalytic reaction model with the assumption that the reactions are first order in methane partial pressure.

Most of the methane is converted in the part of one fourth to one half of the catalyst zone length from inlet to outlet. The temperature gradient between the gas and catalyst surface decreases along the axial distance, and both temperatures approach the same value at the bottom of the catalyst bed. Finally, the results of this simulation have been compared with the industrial data taken from the existing ammonia unit in the State Company of Fertilizers South Region in the Basra/Iraq, which show a relatively good compatibility.

Keywords: Ammonia, Autothermal reformer, Steam reforming, Reforming reactions, Hydrogen production

Background

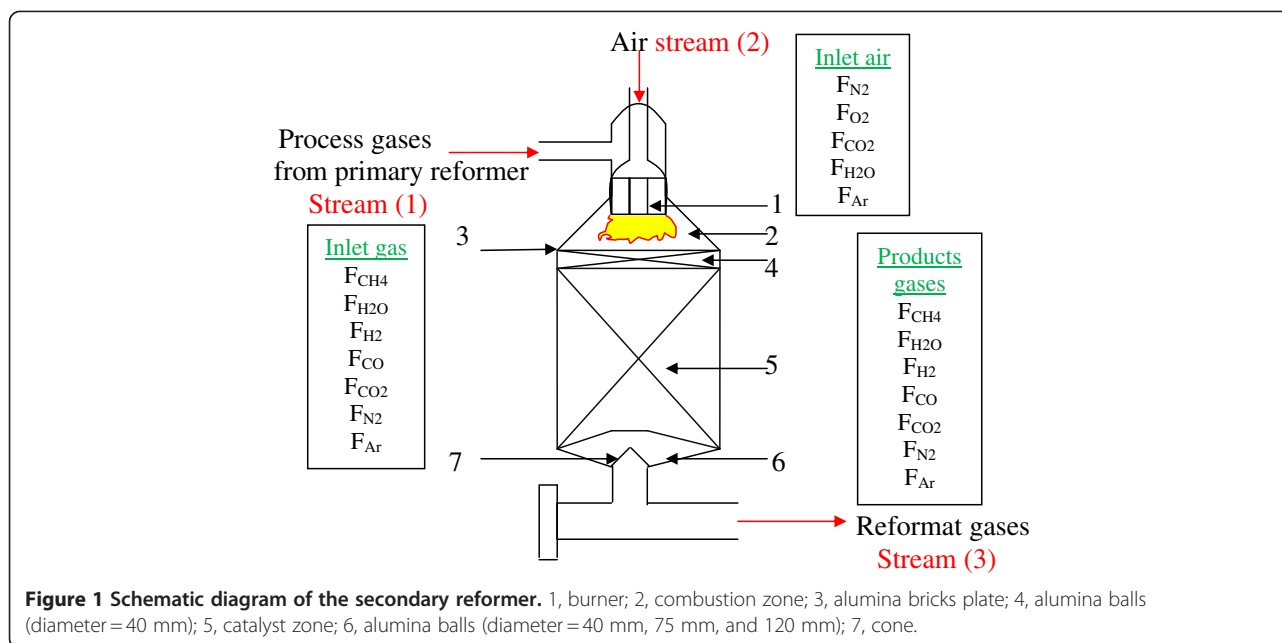
The industrial secondary reformer reactor plays an important role in the ammonia plant. The aim of the secondary reformer reactor is to produce and adjust the amount of hydrogen and nitrogen gases. A schematic diagram of the industrial-scale secondary reformer reactor is shown in Figure 1. The process gas leaves the primary reformer through the transfer line; then, it will enter the secondary reformer at the top through the combustion chamber. Process air is introduced into this combustion chamber, in which the oxygen of the air is burnt, liberating heat and raising the temperature of the product gases from the primary reformer, where N_2 will be produced through this section. The partially oxidized gas passes through the catalyst zone to produce the hydrogen, and it is provided with a Ni/

$MgAl_2O_4$ catalyst inside the reactor shell. Finally, the reformat gases leave the secondary reformer through the outlet nozzle at the bottom of the secondary reformer reactor.

The results of previous studies by various researchers mainly by Ebrahimi et al. [1], Khorsand and Deghan [2], Yu [3], Raghunandaqnan and Reddy [4], and Ravi et al. [5] have included the design and evaluation of the performance of a secondary reformer with different parameters.

Mathematical models which combine the predictions of the overall consumption of the reactants with a prediction of the product distribution are very scarce for the secondary reformer in literature. Only few research groups studied the combustion zone in the secondary reformer reactor explicitly. One reason might be the unavailability of the mechanism of methane and hydrogen combustion in the literature due to the wide distribution of detailed mechanisms for the combustion of

* Correspondence: chemicalengineer82@yahoo.com
Department of Chemical Engineering, Basra University, Basra, 61004, Iraq



natural gas only, which consists mainly of methane. Therefore, numerous researchers focused attention on the autothermal reformer which represented a stand-alone process wherein the entire natural gas conversion is carried out by an internal combustion with oxygen as presented by Amirshaghghi et al. [6], Li et al. [7], Pina and Borio [8], Skukri et al. [9], and Hoang and Chan [10].

Conventional technology employs a single reactor and single nickel catalyst, but in this study, the reactor is divided into two reactors in series. The first reactor, upper section, is the combustion zone that is filled with inert gases from the primary reformer without catalyst; the combustion is carried out by adding an air stream, not oxygen as in the previous studies in autothermal reformer; in the second reactor, bottom section, which is the catalyst zone filled with nickel catalyst, the classic reforming reactions occur. The originality of the work lies in this proposal.

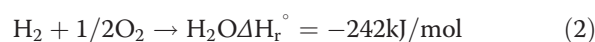
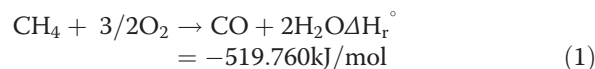
The results of the mathematical model such as mole fraction, temperature profile, and pressure drop of the combustion and catalyst zones will be compared relative to the industrial values taken from the secondary reformer reactor in the State Company of Fertilizers South Region (SCFSR) in the Basra/Iraq to show the degree of accuracy.

Methods

Mathematical model of combustion zone

The homogenous (non-catalytic), exothermic, irreversible reactions take place in the combustion zone. The methane is combusted through numerous radical reactions, but it can be represented as a methane

combustion reaction. Also, H₂ will be converted to H₂O in the combustion zone. The overall reaction mechanism of methane and hydrogen with oxygen in the combustion zone can be considered as follows:



An input–output model of the combustion zone based on global mass and energy balances using a simple mathematical model consists of atomic molar balance and adiabatic flame temperature with the assumption that the feed and inlet air to the reactor are fully mixed along the flame, that complete oxygen consumption is considered, and that the conditions inside and outside of the combustion zone are equal.

For the combustion zone, the atomic molar balance as shown in Figure 1 can be derived as follows:

$$\text{For argon : } F_{\text{IN},1} + F_{\text{IN},2} = F_{\text{OUT}} \quad (3)$$

$$\text{For nitrogen : } F_{\text{IN},1} \times 2 + F_{\text{IN},2} \times 2 = F_{\text{OUT}} \times 2 \quad (4)$$

$$\begin{aligned} \text{For carbon : } & F_{\text{IN}(\text{CH}_4),1} + F_{\text{IN}(\text{CO}),1} + F_{\text{IN}(\text{CO}_2),1} \\ & + F_{\text{IN}(\text{CO}_2),2} \\ & = F_{\text{OUT}(\text{CH}_4)} + F_{\text{OUT}(\text{CO})} \\ & + F_{\text{OUT}(\text{CO}_2)} \end{aligned} \quad (5)$$

$$\begin{aligned} \text{For hydrogen : } & F_{\text{IN}(\text{CH}_4),1} \times 4 + F_{\text{IN}(\text{H}_2\text{O}),1} \times 2 \\ & + F_{\text{IN}(\text{H}_2),1} \times 2 + F_{\text{IN}(\text{H}_2\text{O}),2} \times 2 \\ & = F_{\text{OUT}(\text{CH}_4)} \times 4 + F_{\text{OUT}(\text{H}_2\text{O})} \times 2 \\ & + F_{\text{OUT}(\text{H}_2)} \times 2 \end{aligned} \quad (6)$$

$$\begin{aligned} \text{For oxygen : } & F_{\text{IN}(\text{H}_2\text{O}),1} + F_{\text{IN}(\text{CO}),1} + F_{\text{IN}(\text{CO}_2),1} \\ & \times 2 + F_{\text{IN}(\text{O}_2),2} \times 2 \\ & + F_{\text{IN}(\text{H}_2\text{O}),2} + F_{\text{IN}(\text{CO}_2),2} \times 2 \\ & = F_{\text{OUT}(\text{H}_2\text{O})} + F_{\text{OUT}(\text{CO})} \\ & + F_{\text{OUT}(\text{CO}_2)} \times 2 \end{aligned} \quad (7)$$

$$\begin{aligned} \text{Over all material balance : } & F_{\text{tot}} \\ & = F_{\text{OUT}(\text{CH}_4)} + F_{\text{OUT}(\text{H}_2\text{O})} + F_{\text{OUT}(\text{H}_2)} \\ & + F_{\text{OUT}(\text{CO})} + F_{\text{OUT}(\text{CO}_2)} + F_{\text{OUT}(\text{N}_2)} + F_{\text{OUT}(\text{Ar})} \end{aligned} \quad (8)$$

where $F_{\text{IN},1}$ is the molar flow rate of inlet process gases in the stream number.1 (kmol/h), $F_{\text{IN},2}$ is the molar flow rate of inlet air in the stream number 2 (kmol/h), F_{OUT} is the molar flow rate of each gas from the combustion zone (kmol/h), F_{tot} is the total molar flow rate of outlet gases from the combustion zone (kmol/h).

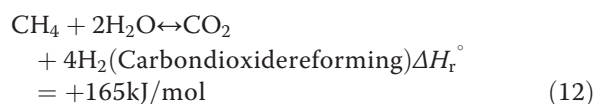
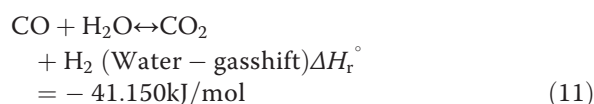
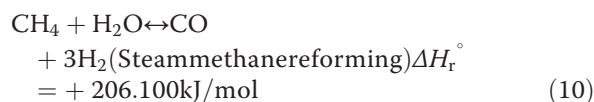
The secondary reformer is operated close to adiabatically, and hence, the temperature is given by the adiabatic heat balance. Adiabatic flame temperature can be described by the following equation:

$$\Delta H = \sum_{\text{OUT}} F_i \cdot H_i - \sum_{\text{IN}} F_i \cdot H_i = 0.0 \quad (9)$$

where, ΔH is the enthalpy change (kJ/kmol), F is the molar flow rate (kmol/h), H_i is the specific enthalpy of the i -component (kJ/kmol).

Mathematical model of catalyst zone

In the catalyst zone, heterogeneous endothermic, reversible reactions take place. The product gas of the combustion zone is directed to the catalytic zone of the secondary reformer. The catalyst bed involves three reversible reactions. Anyway, the following equations can be written as follows:



The reaction rate expressions of Froment and Xu described the kinetic rate of disappearance or

production of species as a function of the partial pressures. The kinetic model of the reactions on a Ni/MgAl₂O₄ catalyst are based on a Langmuir-Hinshelwood reaction mechanism in which rate expressions can be described by the following equations [11]:

$$\begin{aligned} \text{For methane steam reforming reaction(SMR) :} \\ R_1 = k_1 / \left(P_{\text{H}_2}^{2.5} \cdot \text{DEN}^2 \right) \left[P_{\text{CH}_4} \cdot P_{\text{H}_2\text{O}} - (P_{\text{H}_2}^3 \cdot P_{\text{CO}} / K_{e,1}) \right] \end{aligned} \quad (13)$$

$$\begin{aligned} \text{Rateofreactionforwater - gasshiftreaction(WGS) :} \\ R_2 = k_2 / (P_{\text{H}_2} \cdot \text{DEN}^2) \left[P_{\text{CO}} \cdot P_{\text{H}_2\text{O}} - (P_{\text{H}_2} \cdot P_{\text{CO}_2} / K_{e,2}) \right] \end{aligned} \quad (14)$$

$$\begin{aligned} \text{Reaction rate for carbon dioxide reforming} \\ \text{reaction (CDR) :} \\ R_3 = k_3 / \left(P_{\text{H}_2}^{3.5} \cdot \text{DEN}^2 \right) \left[P_{\text{CH}_4} \cdot P_{\text{H}_2\text{O}}^2 - (P_{\text{H}_2}^4 \cdot P_{\text{CO}_2} / K_{e,3}) \right] \end{aligned} \quad (15)$$

where the denominator (DEN) is defined by the following equation:

$$\begin{aligned} \text{DEN} = 1 + K_{\text{ad,CO}} \times P_{\text{CO}} + K_{\text{ad,H}_2} \times P_{\text{H}_2} \\ + K_{\text{ad,CH}_4} \times P_{\text{CH}_4} + K_{\text{ad,H}_2\text{O}} \times P_{\text{H}_2\text{O}} / P_{\text{H}_2} \end{aligned} \quad (16)$$

where R_k is the rate of reaction for reaction k (kmol/kg_{cat}·h), k_k is the constant of reaction rate for reaction k (accordant to the Arrhenius constant), $K_{e,k}$ is the equilibrium constant for reaction k (bar²), $K_{\text{ad},i}$ is the adsorption coefficient of the i -component (accordant to the unit of pre-exponential factor for adsorption of i -component $A_{\text{ad},i}$), DEN is the denominator in the expressions for the reaction rates (dimensionless unit), and P_i is the partial pressure of i -components (bar).

In the heterogeneous reaction, the actual reaction rate is affected by the molecular diffusion into the micropore inside the catalyst. Therefore, the effectiveness factor should be considered in order to apply the kinetic equations to the industrial reactor design. The effectiveness factor can be estimated using the following equation as noted by Froment and Bischoff [12]:

$$\eta_k = (1/\phi_k) \left((1/\tanh(3\phi_k)) - (1/3\phi_k) \right) \quad (17)$$

where η_k is the reaction effectiveness factor for reaction k (dimensionless unit) and the Φ Thiele modules (dimensionless unit).

The spherical catalyst pellet is assumed to find the effectiveness factor to apply on the design of the industrial catalytic reformer. If the catalyst pellet is spherical, the Thiele Modulus can be defined by the following equation with a characteristic length, $D_s/6$, as noted by previous researchers including Rostrup-Nielsen and Froment and Bischoff [12]:

$$\phi_k = \frac{D_s}{6} \sqrt{\frac{k_{v,k} \cdot \rho_b \cdot (1 + K_{e,k})}{K_{e,k} \cdot D_{e,k}}} \quad (18)$$

where D_s is the equivalent pellet diameter (m). This is defined as the diameter of a sphere with the same external surface area per unit volume of the catalyst pellet, $D_s = 6 \cdot (1 - \epsilon_B) / S_B$; where, the S_B is the specific surface area of bed (m^3/m^2) and, the S is the specific surface area of pellet (m^2/m^3), the A_p is surface area of pellet while, v_p is the volume of pellet ϵ_B is the porosity of packed bed ($\text{m}^3_{\text{void}}/\text{m}^3$). $k_{v,k}$ is the volumetric kinetic constant for reaction k (to convert the unit of constant of reaction rate) ($\text{m}^3/\text{Kg}_{\text{cat}} \cdot \text{h}$). ρ_b is the bulk density (kg/m^3). The effective diffusivity of the i -component for reaction k is defined as follows [3]:

$$D_{e,k} = 1 / \left[(1/D_{Kn,i}) + (1/D_{i,mix}) \right] \quad (19)$$

where $D_{e,k}$ is the effective diffusivity of reaction k (m^2/h). $D_{i,mix}$ is the molecular diffusivity of the i -component (m^2/h). $D_{Kn,i}$ is the Knudsen diffusivity (m^2/h).

In the secondary reformer reactor, the gas product from the combustion zone is directed to the catalyst bed, while the catalytic reactions as shown in Equations 10, 11, and 12 take place on the nickel catalyst. Therefore, the mass balance for i -component and heat balance in axial direction based on an adiabatic one-dimensional heterogeneous catalytic reaction model can be described by the following equation [3]:

$$\left(\partial F_i / \partial \ell \right) = \sum_{k=1}^3 v_{i,k} \cdot \eta_k \cdot R_k \cdot \rho_C \cdot (1 - \epsilon_B) \cdot A \quad (20)$$

where ℓ corresponds to axial coordinates (m) and v_i is the stoichiometric coefficient of the i -component in the chemical reaction equations (dimensionless unit). ρ_C is the density of catalyst (kg/m^3), A is the cross section area (m^2). The change in the temperature throughout the reactor length has been given as follows [12]:

$$F_g \cdot C_{p,g} \cdot \rho_g \cdot \left(\partial T_g / \partial \ell \right) = \sum_{k=1}^3 \left(-\Delta H_{r,k}^\circ \right) \cdot \eta_k \cdot R_k \cdot \rho_C \cdot (1 - \epsilon_B) \cdot A \quad (21)$$

where F_g is the molar flow rate of gases in the catalyst zone (kmol/h), C_p is the specific heat capacity ($\text{kJ}/\text{kmol} \cdot \text{K}$), T is the temperature of gases (K), $\Delta H_{r,k}^\circ$ is the standard heat of reaction k (kJ/mol), and ρ_g is the density of gases (kg/m^3).

The temperature of the catalyst surface is a very important factor in heterogeneous reactions. It was evaluated relative to the bulk gas temperature [3].

$$T_s = T_g + \frac{\left(\left(\sum (-\Delta H_{r,k}^\circ) \cdot \eta_k \cdot R_k \right) \cdot \rho_C \cdot (1 - \epsilon_B) \cdot D_s \right)}{(6 \cdot h \cdot (1 - \epsilon_B))} \quad (22)$$

where T_s is the temperature surface of the catalyst (K) and h is the heat transfer coefficient ($\text{kJ}/\text{m}^2 \cdot \text{K} \cdot \text{h}$) which is represented as $h = (\text{Nu} \cdot K / D_s)$.

The thermal conductivity could be estimated from the following equation [13]:

$$K = \mu_g \left(C_{p,g} + (10.4 / M_{wt,i}) \right) \quad (23)$$

where K is the thermal conductivity of gases ($\text{W}/\text{m} \cdot \text{K}$), C_p is the specific heat capacity ($\text{kJ}/\text{kg} \cdot \text{K}$), M_{wt} is the molecular weight of gases (kg/kmol), and μ_g is the viscosity of gases ($\text{Pa} \cdot \text{s}$).

For the packed bed, the Nusselt number equation could be formulated by the following equation [14]:

$$\text{Nu} = 2.0 + 1.3 \text{Pr}^{0.15} + 0.66 \text{Pr}^{0.31} \text{Re}_p^{0.5} \quad (24)$$

where Nu is the Nusselt number (dimensionless unit), Pr is Prandtl's number (dimensionless unit), and Re_p is the Reynolds number of a particle (dimensionless unit).

For the flow through ring packing often used in industrial packed columns, the Ergun equation is considered as a good semi-empirical correlation for predicting pressure drop as follows [14]:

$$\frac{\partial P}{\partial \ell} = - \left(\left((150(1 - \epsilon_B)^2 \cdot \mu_g \cdot u) / (\epsilon_B^3 \cdot D_s^2) \right) + \left((1.75 \cdot (1 - \epsilon_B) \rho_b \cdot u^2) / (\epsilon_B^3 \cdot D_s) \right) \right) \quad (25)$$

where P is the pressure of gases (bar), u is the velocity of gases (m/h) $u = Q/A$, and Q is the volumetric flow rate (m^3/h).

Solution procedure

The solution starts with an assumption of the initial total molar flow rate of outlet gases (F_{tot}) of the combustion zone. Chemical compositions and temperature are calculated using the atomic molar balance and the adiabatic flame temperature equations. Consequently, the final calculation results will be used as input data to the catalytic zone. The reaction rate equations are used with mass and heat balance to determine the temperature and composition profile for each component as a function of reactor length in the catalyst zone. The set of differential equations will be solved using the numerical analysis, Euler method. The iteration calculation will apply and repeat until the molar fraction calculation and reaction temperature will agree with the industrial value. Otherwise, a new guessing value of the total molar flow rates of outlet gases from the combustion zone will be assumed.

Results and discussion

Combustion zone

The actual operating conditions such as feed molar flow rate, temperature, and pressure have been tabulated in Table 1. These data are used for modeling and evaluating the theoretical performance of the industrial secondary reformer reactor.

Table 1 Actual operations conditions of industrial secondary reformer in SCFSR in Basra/Iraq [15]

Parameters	Input feed process gas Stream 1	Input air Stream 2
Temperature (°C)	795	550
Pressure (bar)	32	32
Molar flow rates of the components (kmol/h)		
CH ₄	426.040	-
H ₂ O	3,684.010	11.190
H ₂	2,932.100	-
CO	403.460	-
CO ₂	537.440	0.520
N ₂	15.990	1,357.360
Ar	5.830	16.350
O ₂	-	365.080

Table 2 Output data of the industrial secondary reformer and simulation [15]

Parameters	Output of combustion zone (simulation data)	Output of secondary reformer (simulation data)	Output of secondary reformer (plant data)
Temperature (°C)	1,096.644	1,009.630	969
Pressure (bar)	32	31.918	31.570
Mole flow rates (kmol/h) of the components			
CH ₄	183.698	19.001	18.640
H ₂ O	4,182.983	3,985.640	3,992.350
H ₂	2,929.004	3,455.730	3,449.710
CO	645.806	777.861	785.200
CO ₂	537.947	570.589	563.600
N ₂	1,373.380	1,373.380	1,373.360
Ar	22.180	22.180	22.180
O ₂	-	-	-
Total molar flow rate (kmol/h)	9,875	10,204.400	10,205.504
H ₂ /N ₂	2.132	2.516	2.511
(CO + H ₂)/N ₂	2.602	3.082	3.083

According to the simulation results of the mathematical model, the temperature of the combustion chamber is 1,096.644°C. The values of the components' molar flow rate have been given in Table 2, as there are no industrial data available in this zone; therefore, they are not comparable.

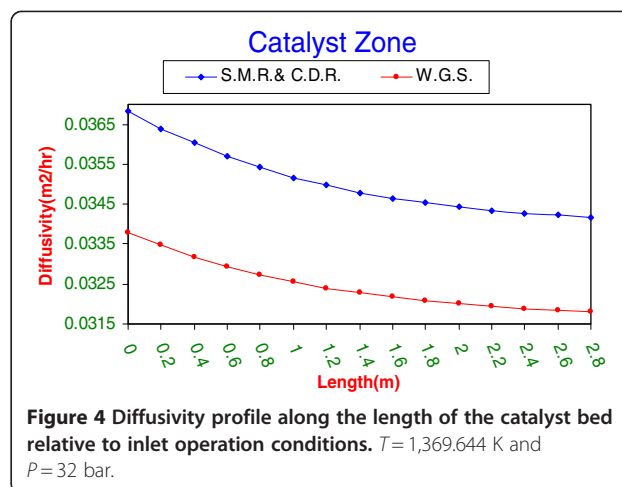
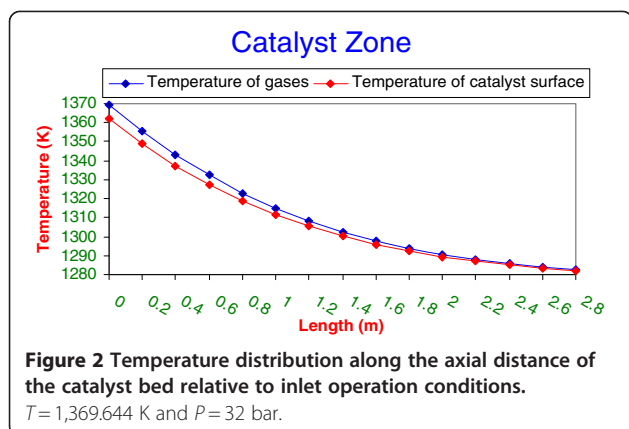
Catalyst zone

In this section, the influence of temperature has been discussed for describing the effect of these parameters on the design of the secondary reformer relative to Basra Fertilizer Plant.

Figure 2 depicts the profile of temperature gases and catalyst surface as a function of reactor length. The sharp decline along the reactor occurred due to the general behavior of methane steam reforming, and carbon dioxide reforming reactions are prevailing endothermic reforming reactions that control the reaction pathway, while the water-gas shift reaction is a slightly exothermic reaction. The profile of gas and catalyst temperatures is a very important parameter effect on the rates of chemical reactions.

In the region of the catalyst entrance, the rate of reactions for methane steam and carbon dioxide reforming reactions is very fast. This is due to the higher effect of operation conditions such as partial pressure of methane and the value of feed temperature. After the middle of the catalyst zone, the trend of reaction rates in the Figure 3 has declined slowly due to the effect of endothermic reactions relative to chemical reactions in Equations 10 and 12. The reforming reaction rates at the inlet catalyst zone are considerably higher than the water-gas shift reaction because the last reaction became more active under a low temperature range; then, in middle of the catalyst zone it begins to increase because the temperature becomes low [9]. The water-gas shift reaction is negative along the axial distance from the top of the bed due to inversion of the water-gas shift reaction inside the catalyst particles [8].

Figure 4 depicts the decline of diffusivities along the reactor length due to the diffusion phenomena that occurred from high to low concentration regions (concentration gradient). Also, there are other driving forces (besides concentration differences) such as temperature and pressure gradients [16]. The overall reaction rate is mainly controlled by the diffusion rate due to the rate of mass transfer (diffusivity) of the reactants to the catalyst pellet which is low; the concentration of reactants in the catalyst pellet will be low because it is consumed by the reaction as fast as it arrives [17] so that the conditions' mean reaction occurs before the reactant has diffused far into the pellet [12].



The effectiveness factor is an important parameter to predict the temperature and composition profiles for realizing the actual reaction rate with pore diffusion.

In this study, the effectiveness factors show low values ranging from 0.006 to 0.001 along the axial distance of the catalyst bed as shown in Figure 5 due to many factors such as large pellets, low diffusivity, and high values of the constant rate of reactions. Note that the effectiveness factor $\ll 1$ means that only the surface near to the outer surrounding of the pellet is effective. In this case, the catalyst in the central portion of the pellet is not utilized [12].

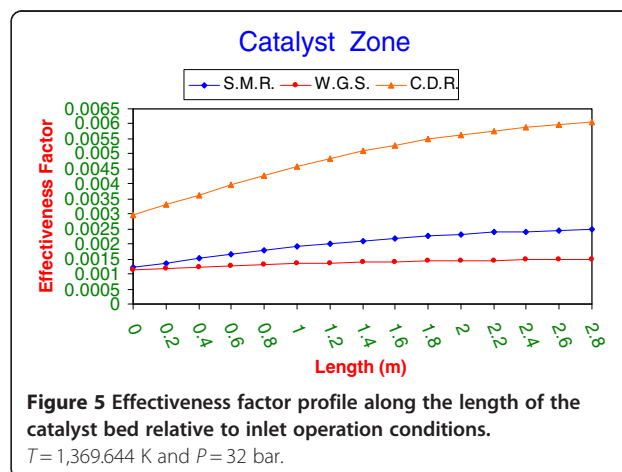
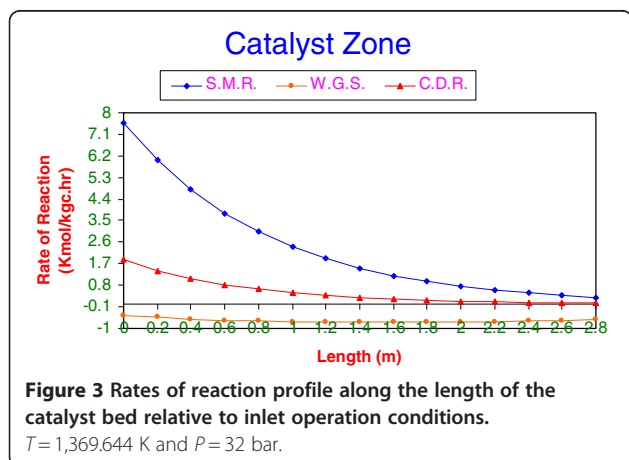
The theoretical results' prediction from the mathematical model has been compared with the industrial data collected from the manual and daily log sheet of the Basra Fertilizer Plant as summarized in Table 2. The results depicted high accuracy between simulation results and plant data.

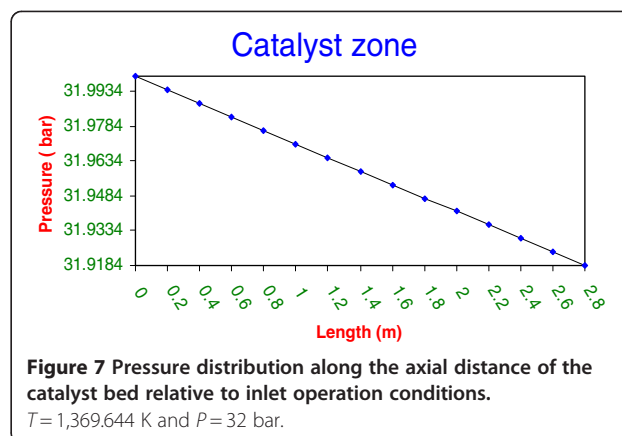
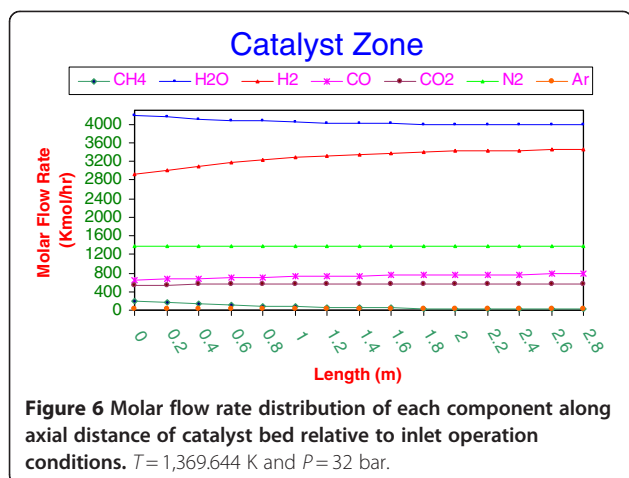
Figure 6 depicts the molar flow rate distribution of each component along the axial distance of the catalyst bed. Methane is almost completely consumed at inlet

conditions of the catalyst bed due to the high temperature of gases coming from the combustion zone. High temperature accelerates the reaction rates of steam methane reforming and carbon dioxide reforming. Most of the methane conversion had been achieved in the half of the catalyst bed. Then, the rate of reactions of the methane steam reforming and carbon dioxide reforming has been decreased as shown in Figure 3 because the temperature and partial pressure of methane had been decreased.

The sharp increase in the H_2 content is mainly explained by SMR and CDR as shown in Figure 3 along the catalyst bed. Thus, the hydrogen production is dominated by chemical reactions in Equations 10 and 12.

The sharp increase in CO along the reactor length occurred due to the methane steam reforming and water-gas shift reactions as shown in Figure 3 relative to the chemical reactions in Equations 10 and 11.





The CO_2 generation is described by the reactions of water-gas shift and carbon dioxide reforming as mentioned in Equations 11 and 12. The increase in CO_2 production occurred due to carbon dioxide reforming as shown in Figure 3. Then, the decline occurred due to CO_2 which was consumed by the water-gas shift reaction because of the inversion of the water-gas shift reaction inside the catalyst particles. (It's negative along the axial distance from the top of the bed). Nitrogen and argon are constant along the reactor length because neither nitrogen nor argon reacted with any other components.

In the gas phase of the packed bed catalytic reaction system, pressure drop is one of the important parameters. From a practical point of view, the value of the pressure drop gives a good indication about catalyst performance inside the reaction shell. There are many reasons for the increase of pressure drop, for example, with a long time of operation; the catalyst may be thermal cracking due to the high operation temperature, so the value of pressure drop will increase.

The decline of pressure along the reactor occurred due to the friction between particles of gases, particles of gases with pellets of the catalyst, and particles of gases with a wall of reactor as shown in Figure 7.

Experimental

In this section, the analysis of inlet and outlet synthesis process gases for the industrial secondary reformer reactor in Basra Fertilizer Plant has been carried out. The experimental part will investigate, specify, and tabulate the actual operation conditions of the industrial secondary reformer as summarized in Table 1.

Currently, describing the industrial secondary reformer reactor at Basra Fertilizer Plant, the industrial catalyst and the operation conditions must be understood with more details.

The wall of the secondary reformer is fabricated from carbon steel with three refractory layers that are lined to protect the wall and to reduce the heat loss. The inside diameter of the secondary reformer is 3.450 m with a lining thickness of 440 mm. The alumina brick plate is located above the catalyst bed in order to distribute the combusted gas evenly to the catalyst bed. The alumina balls of 40 mm in diameter are packed below the alumina brick plate with a depth of 300 mm and with a volume of 2.500 m^3 to protect the catalyst. The nickel catalysts, RKS-2, with one hole are packed with a volume of 26 m^3 ; the height of the catalyst bed is 2.8 m as depicted in Table 3. The catalyst is supported by a ceramic ball and cone made of high alumina bricks which are comprised of bricks with slot holes that provide a highly stable support for the catalyst which bears the catalyst weight. The catalyst support is covered with alumina balls of 40 mm with heights of 300 mm, 75 mm, and 120 mm and with volumes of 2.800, 4.100, and 4.100 m^3 , respectively.

Conclusion

The secondary reformer for hydrogen and nitrogen production is mathematically investigated by a series of

Table 3 Physical characteristic of the catalyst [15]

Catalyst pellet	
Model name	RKS-2
Shape	Rings
Nominal Size: OD × ID × H	19 × 9 × 19 mm
Chemical composition	
NiO wt. %	9%
MgAl ₂ O ₄ wt. %	Balance
Filling density	1.070 Kg/L

OD, outer diameter; ID, inner diameter; H, height.

simulation of operation conditions which have been collected from the documents of Basra Fertilizer Plant.

A mathematical model of the industrial secondary reformer in Basra Fertilizer Plant with all assumptions made had been completed. The theoretical results obtained have been compared with the industrial secondary reformer reactor details. The results show a good compatibility as shown in Table 2. The model predicts the temperature and composition profiles of the gas that leaves the combustion chamber and investigates the temperature and concentration gradient inside the catalyst particle. The value of pressure drop depicts low values along the axial distance of the catalyst bed; therefore, pressure drop can be assumed negligible. The overall reaction rate is mainly controlled by the diffusion rate. In the catalyst zone entrance, methane steam reforming and carbon dioxide reforming reaction rates at the catalyst zone inlet were considerably higher than the water-gas shift reaction. The diffusion into the pellet is relatively slow so that these conditions' mean reaction occurs before the reactant has diffused far into the pellet. The effectiveness factor $\ll 1$ means that only the surface near from the outer surrounding of the pellet is effective; therefore, the diffusion and effectiveness factor gave a good indication about the shape of the catalyst that is used in the catalyst zone as a ring without a central portion because the chemical reaction takes place at the outer surface. Finally, this simulation model depicts a high reliability for the designing and testing of an industrial secondary reformer, not for Basra Fertilizer Plant, but it is extended to any secondary reformer reactor in fertilizer plants.

Abbreviations

CDR: carbon dioxide reforming reaction; SCFSR: State Company of Fertilizers South Region; SMR: methane steam reforming reaction; WGS: water-gas shift reaction.

Acknowledgement

We acknowledge the full cooperation of the State Company Fertilizer Plant South Region in Basra/Iraq to introduce the industrial data for this investigation.

Received: 26 February 2012 Accepted: 29 May 2012

Published: 19 July 2012

References

1. Ebrahimi H, Behroozsarand A, Zamaniyan A (2010) Arrangement of primary and secondary reformers for synthesis gas production. *Chemical Engineering Research and Design* **88**:1342–1350
2. Khorsand K, Deghan K (2007) Modeling and simulation of reformer autothermal reactor in ammonia unit. *Petroleum and Coal* **49**:64–71
3. Yu YH (2002) Simulation of secondary reformer in industrial ammonia plant. *Chem Eng Tech J* **25**:307–314
4. Raghunandan KS, Reddy KV (1994) Development of a mathematical model for a secondary reformer. *Chem Eng. Tech J* **17**:273–279
5. Ravi K, Dhingra SC, Guha BK, Joshi YK (1989) Simulation of primary and secondary reformers for improved energy performance of an ammonia plant. *Chem Eng Tech J* **12**:358–364
6. Amirshaghghi H, Zamaniyan A, Ebrahimi H, Zarkesh M (2010) Numerical simulation of methane partial oxidation in the burner and combustion

- chamber of autothermal reformer. *Applied Mathematical Modeling* **34**:2312–2322
7. Li Y, Wang Y, Zhang X, Mi Z (2008) Thermodynamic analysis of autothermal steam and CO₂ reforming of methane. *International Journal of Hydrogen Energy* **33**:2507–2514
8. Pina J, Borio DO (2006) Modeling and simulation of an autothermal reformer. *Latin American Applied Research J* **36**:289–294
9. Shukri MI, Songip AR, Ahmad A, Nasri NS (2004) Simulation study of methane autothermal reforming for hydrogen production. In: *Proceedings of Advances in Malaysian fuel cell research and development*, pp p149–p158
10. Hoang DL, Chan SH (2004) Modeling of a catalytic autothermal methane reformer for fuel cell applications. *Applied Catalysis J* **268**:207–216
11. Xu J, Froment GF (1989) Methane steam reforming: II. Diffusional limitations and reactor simulation, *AIChE J.* **35**
12. Smith JM (1970) *Chemical engineering kinetics*. Chemical engineering series, McGraw-Hill; New York
13. Sinnott RK (1999) *Unit operations*. In Related Butterworth-Heinemann titles in the chemical engineering series, vol.6, 3rd edition., Butterworth-Heinemann, Oxford
14. Coulson JM, Richardson JF, Bucharust JR, Harker JH (2002) *Unit operations*. In Related Butterworth-Heinemann titles in the chemical engineering series, vol 2, 5th edition., Butterworth-Heinemann, Oxford
15. Documents of State Company of Fertilizer Plant South Region
16. Geankoplis CJ (1983) *Transport processes and unit operation*. Prentice Hall Professional Technical Reference, New Jersey
17. Luyben W (1996) *Process modeling, simulation, and control for chemical engineers*, 2nd edition, Mc Graw Hill; New York

doi:10.1186/2228-5547-3-14

Cite this article as: AL-Dhfeery and Jassem: Modeling and simulation of an industrial secondary reformer reactor in the fertilizer plants. *International Journal of Industrial Chemistry* 2012 **3**:14.

Submit your manuscript to a SpringerOpen[®] journal and benefit from:

- Convenient online submission
- Rigorous peer review
- Immediate publication on acceptance
- Open access: articles freely available online
- High visibility within the field
- Retaining the copyright to your article

Submit your next manuscript at ► springeropen.com